Finite Difference Time Domain Modeling of Fringe Waves

Mehmet Alper Uslu [1], Gokhan Apaydin [2], and Levent Sevgi [3]

[1] Department of TGE, NETAS, Istanbul, Turkey
auslu@netas.com.tr

[2] Electromagnetic Consulting, Istanbul, Turkey
g.apaydin@gmail.com

[3] Department of Electrical-Electronics Engineering
Okan University, Tuzla, Istanbul, 34759, Turkey
levent.sevgi@okan.edu.tr

Abstract ─ A novel method is introduced for calculating fringe currents and fringe waves around the tip of a perfectly reflecting wedge under line source illumination. The time-domain fringe (non-uniform) currents are extracted with the finite-difference time-domain (FDTD) method. These currents are then fed into a free-space FDTD and fringe waves are excited. Alternatively, fringe waves are also obtained using the Green's function approach. The validation of the proposed method and the verification of the results are done against the physical theory of diffraction (PTD) as well as the method of moments (MoM). The factors affecting the accuracy are also discussed.

Index Terms ─ Finite difference time domain (FDTD), fringe waves, method of moments (MoM), nonuniform currents, physical theory of diffraction, PTD, uniform currents, wedge.

I. INTRODUCTION

Physical optics (PO), introduced by Macdonald in 1912, is a high frequency asymptotic (HFA) technique used for the calculations of scattered fields from perfectly electrical conducting (PEC) objects [1]. PO is a source-based technique where currents are assumed to be induced on an infinite PEC plane tangent to the object. PO source induced currents, which are nonzero only on the illuminated side of object's surface (away from any discontinuity), are named as uniform currents. PO-based scattered fields, which consist of reflected and diffracted fields, yield inaccurate results for the objects having discontinuities such as sharp edges and/or tips. This is because the magnitude of the induced currents near a discontinuity is not uniformly distributed. In other words, diffraction is not modeled properly with PO's uniform current approximation. Physical theory of diffraction (PTD) extends PO by introducing fringe (non-uniform) currents. The PTD scattered fields contain contributions of both uniform (PO) currents and non-uniform (fringe) currents [2]. The fields radiated from fringe currents are called fringe waves.

The understanding and investigation of fringe waves are critical in broad range of electromagnetic (EM) problems, such as radar cross-section, propagation, electromagnetic compatibility modeling and simulation. The canonical wedge structure has long been used for this purpose. For example, exact and asymptotic formulations of fringe currents are given for a PEC wedge illuminated by a plane wave in [3] and for the line source illumination in [4]. A novel method of moments (MoM)-based approach is also introduced recently [5]. Finite difference time domain (FDTD) is a numerical method used in solving Maxwell's equations in time domain. It has been widely used in variety of EM problems including radiation, propagation, and scattering. The FDTD method has also been used in the calculation of diffraction coefficients and there are many studies in modeling diffraction from various wedges [6]–[9]. Recently, double tip diffraction has also been modeled with FDTD [10]. Here, we propose a novel FDTD method for the extraction of fringe currents and fringe waves on the canonical PEC wedge structure. The fringe fields are also computed via Green's function based on FDTD-extracted fringe currents.

The paper is organized as follows. In Section 2, we describe the problem and summarize PTD fringe wave expressions. Then, the FDTD-based fringe currents extraction procedure is outlined in Section 3. Section 4 presents examples and numerical comparisons against the PTD and MoM data. Conclusions are given in Section 5.

II. GEOMETRY OF THE PROBLEM

The geometry of the problem is shown in Fig. 1.

Submitted On: November 12, 2016
Accepted On: January 28, 2017

Here, a PEC wedge with apex angle $2\pi-\alpha$ is illuminated by a line source located at (ρ_0,φ_0). The tip of the wedge is at the origin. The receiver is at (ρ,φ). The incident EM wave hits the wedge and induces surface currents. This induced current consists of uniform (PO) and non-uniform (fringe) parts [2]. Non-uniform currents cause fringe waves.

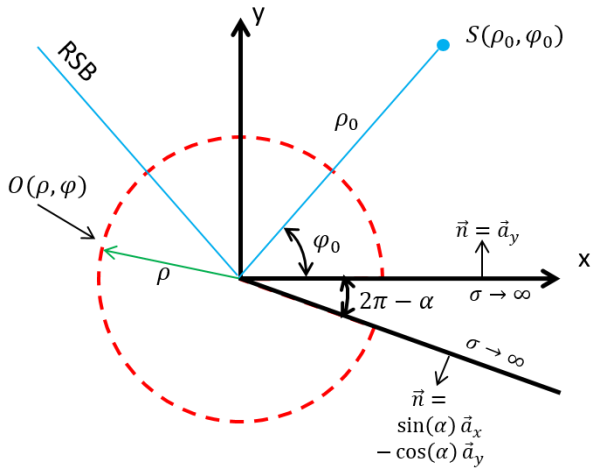

Fig. 1. Geometry of the problem under SSI illumination.

PTD fringe fields are obtained by subtracting PO diffracted fields from total/exact diffracted fields:

$$u^{fringe}=u^{d,Exact}-u^{d,PO}. \tag{1}$$

Exact diffracted fields can be obtained from both integral and series summation representations [2, 3, 11]. Below, the integral solution is given for the sake of completeness for both soft (TM) and hard (TE) boundary condition (BC), respectively:

$$\begin{aligned}u_s^d=&\{V_d(-\pi-\varphi+\varphi_0)-V_d(\pi-\varphi+\varphi_0)\}\\&-\{V_d(-\pi-\varphi-\varphi_0)-V_d(\pi-\varphi-\varphi_0)\},\end{aligned} \tag{2}$$

$$\begin{aligned}u_h^d=&\{V_d(-\pi-\varphi+\varphi_0)-V_d(\pi-\varphi+\varphi_0)\}\\&+\{V_d(-\pi-\varphi-\varphi_0)-V_d(\pi-\varphi-\varphi_0)\},\end{aligned} \tag{3}$$

where

$$V_d(\beta)=\frac{1}{2\pi n}\int_0^\infty H_0^{(1)}[kR(it)]\frac{\sin(\beta/n)}{\cosh(t/n)-\cos(\beta/n)}dt, \tag{4}$$

with $n=\alpha/\pi$ and $R(\eta)=\sqrt{r^2+r_0^2+2rr_0\cos(\eta)}$. PO diffracted fields are given as [4]:

$$u_{s,h}^{d,PO}(r,\varphi)=u^{d,inc}+u_{s,h}^{d,refl}, \tag{5}$$

where

$$u^{d,inc}(r,\varphi)=\frac{kr\sin(\varphi-\varphi_0)}{4i}\int_0^\infty H_0^{(1)}[k(r_0+r')]H_1^{(1)}(k\rho^-)\frac{dr'}{\rho^-}, \tag{6}$$

with $\rho^-=\sqrt{r^2+r'^2+2rr'\cos(\varphi-\varphi_0)}$ and,

$$u_s^{d,refl}(r,\varphi)=-\frac{kr\sin(\varphi+\varphi_0)}{4i}\int_0^\infty H_0^{(1)}[k(r_0+r')]H_1^{(1)}(k\rho^+)\frac{dr'}{\rho^+}, \tag{7}$$

with $\rho^+=\sqrt{r^2+r'^2+2rr'\cos(\varphi+\varphi_0)}$. The term $u_h^{d,refl}$ is used for hard BC and expressed by the opposite of (7). Numerical computation of this integral representation is discussed in [12].

III. FDTD MODELING OF FRINGE WAVES

FDTD is a numerical method which is based on discretization of Maxwell's equations in both space and time. The first and most popular (staircase) discretization scheme was proposed by Yee in 1966 [13]. In this scheme, field components are assumed to be located in space as shown in Figs. 2 and 3. Besides the spatial difference, electric and magnetic fields are also assumed to be separated in the time domain by a half-time step. The 2D FDTD equations, for the scenario in Fig. 1, corresponding to soft (TM_z) and hard (TE_z) BC problems contain (H_x, H_y, E_z) and (E_x, E_y, H_z) components, respectively.

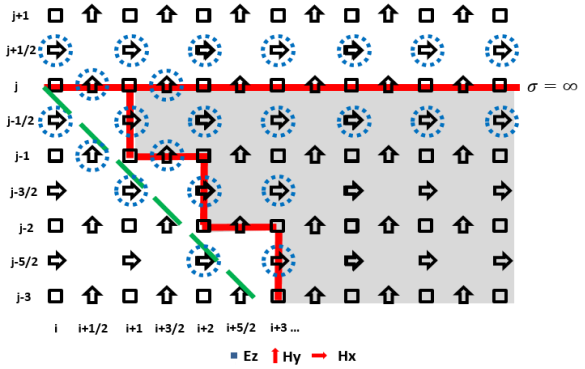

Fig. 2. A FDTD model of the problem in the TMz configuration. The magnetic field components used for calculation of surface currents are circled.

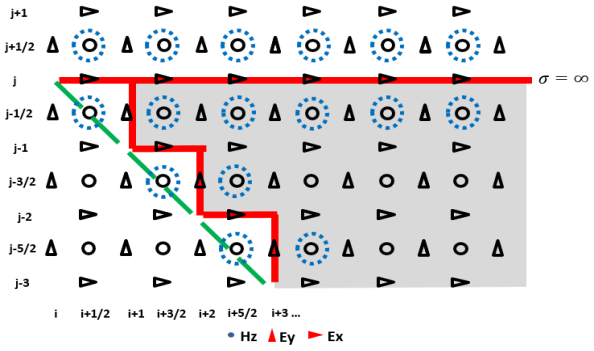

Fig. 3. A FDTD model of the problem in the TEz configuration. The magnetic field components used for calculation of surface currents are circled.

The PEC wedge in TM_z configuration is modeled by setting all electric field components to zero for the cells lying inside. For TE_z configuration, the electric field components lying inside are set to zero and the magnetic fields are updated in the usual way.

The source-induced surface currents are modeled using the tangential magnetic fields. On the top surface and for the TMz mode, this is expressed by:

$$\vec{J}_s^{top} = \hat{a}_y \times \vec{H} = -\hat{a}_z H_x . \quad (8)$$

The field components are not collocated because of the staggered nature of FDTD grid. Hence, spatial averaging can be applied to magnetic fields for approximating their values on the boundaries. As shown in Fig. 2, H_x components are positioned a half-cell ($\Delta y/2$) above and below of top surface; these are used in averaging source-induced surface currents. The bottom surface is not that simple because the normal direction changes according to the position of the E-field. For example, the surface normal is directed along $-\hat{a}_x$ for the boundary between nodes $(i+1, j)$ and $(i+1, j-1)$. Hence, source-induced surface current is obtained by averaging four H_y located around the boundary, i.e.:

$$\vec{J}_s^{bot,TM_z}(n,1) = 0.25\begin{bmatrix} H_y(i+1/2, j-1) + H_y(i+1/2, j) \\ + H_y(i+3/2, j-1) + H_y(i+3/2, j) \end{bmatrix}, \quad (9)$$

where n is time index. For TE_z mode, H_z is used in obtaining source-induced surface currents on both top and bottom surfaces. As seen in Fig. 3, spatial averaging is also required for this mode.

The novel multi-step FDTD approach used for the calculation of fringe currents and fringe waves in the time domain is as follows:

- Run the FDTD simulation for the PEC wedge structure and record surface currents in the time domain. On the top surface, recorded currents contain both uniform and non-uniform parts; on the bottom surface it contains only non-uniform currents.
- Make the wedge angle 180° (i.e., replace wedge with the half-plane), run the FDTD simulation again, and record surface currents only on the top surface of the wedge. Recorded data contains only uniform (PO) currents.
- Subtract data recorded in Step 2 from Step 1 and obtain only non-uniform currents on the top surface.
- Remove the wedge from the FDTD space, use discrete form of $\nabla \times \vec{H} = \varepsilon_0 \partial \vec{E}/\partial t + \vec{J}$ equation and feed the time-domain fringe current using $\vec{J}$ to the related E-field component(s) and run the FDTD program. The FDTD simulation directly yields the fringe waves.

Note that, this procedure is for single side illumination (SSI) as shown in Fig. 1. For the double-side illumination (DSI), where both faces of wedge are illuminated by the incident field, uniform currents are also induced on the bottom surface; hence one additional step, which is similar to Step 2, needs to be performed. In this step, the bottom surface of the wedge is extended to infinity and the time domain currents are recorded. The recorded currents are formed by only uniform currents and they need to be subtracted from the total currents obtained in step 1 on bottom surface.

Note also that, frequency domain fringe currents (at a specified frequency) may also be obtained using FFT. Fringe waves may then be calculated analytically using the Green's function representations, for example, as in (6a) and (6b) in [10] for the TE and TM modes, respectively.

IV. EXAMPLES AND COMPARISONS

The proposed approach is validated and verified against PTD and MoM through the examples presented in Figs. 4-11. Here, different wedge angles (0°, 45°, and 90°) and different angle of illuminations are used. The frequency is 30 MHz.

In Fig. 4, TM_z fringe fields around a 90° PEC wedge, illuminated by a line source at ρ_0=60 m, φ_0=70° recorded on a circle with a radius 20 m (2λ) from the tip are shown. Note that, Fig. 4 (a) shows angular variation of the fringe fields in the frequency domain, while Fig. 4 (b) shows a snapshot during the FDTD simulations (i.e., time-domain pulsed fringe fields).

Time domain characteristics of PO and fringe currents, recorded on the top surface of this wedge at a point 1.5 m away from the tip, are shown in Fig. 5. Normalized frequency domain variations of the same point are also shown in Fig. 6 with source's FFT.

The total (uniform + non-uniform) and non-uniform currents induced on this PEC wedge are shown in Fig. 7. As observed, non-uniform currents concentrate in the vicinity of edge. Figures 8 and 9 belong to the same scenario but for the TE_z polarization.

The simulations are repeated for 0° and 45° PEC wedges and results are presented in Figs. 10 and 11. As observed, very good agreement among analytical and numerical methods are achieved.

Note that, FDTD simulations are performed on a 400×400 cell area. The spatial resolution is $\Delta x = \Delta y = \lambda/20$ corresponds to 0.5 m cell size at 30 MHz. Temporal resolution is $\Delta t = 1.18$ ns. Once-differentiated Gaussian pulse is used as the excitation $\sqrt{2e}(n\Delta t - t_0)/\tau\, e^{-(n\Delta t - t_0)^2/\tau^2}$. Here, n is time-step, $\tau = \sqrt{2.3}/\pi f_0 \approx 0.16$ ns is the characteristics-half width and $t_0 = 4.5\tau$ is temporal delay. The discretization of the PTD and MoM are as in [4] and [5], respectively.

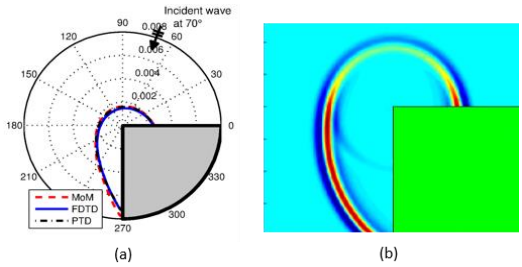

Fig. 4. (a) Fringe fields around the tip of the wedge for TM_z polarization (SSI), Dashed: MoM, Solid: FDTD, Dashed-dotted: PTD, α=270°, ρ_0=60 m, φ_0=70°, ρ=20 m, f=30 MHz; (b) a time-domain snapshot showing broad-band fringe fields.

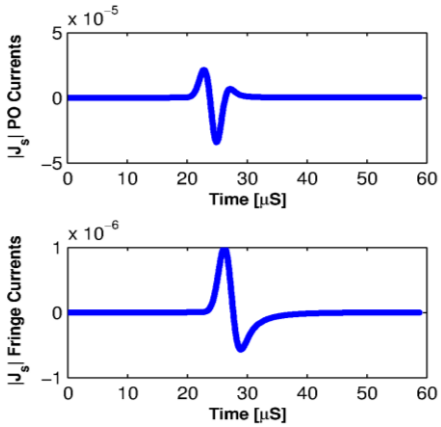

Fig. 5. Time domain surface currents for TM_z polarization of above scenario recorded on top surface at 1.5 m distance from the tip, (Top) PO currents, (Bottom) fringe (non-uniform) currents, α=270°, ρ_0=60 m, φ_0=70°, ρ=20 m, f=30 MHz.

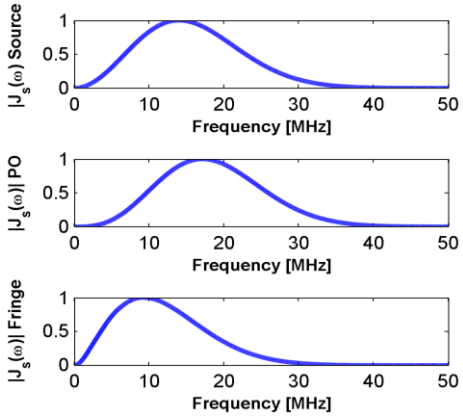

Fig. 6. Normalized frequency domain surface currents for TM_z polarization of above scenario recorded on top surface at 1.5 m distance from the tip, (Top) Source's FFT, (Middle) FFT of PO currents, (Bottom) FFT of fringe (non-uniform) currents, α=270°, ρ_0=60 m, φ_0=70°, ρ=20 m, f=30 MHz.

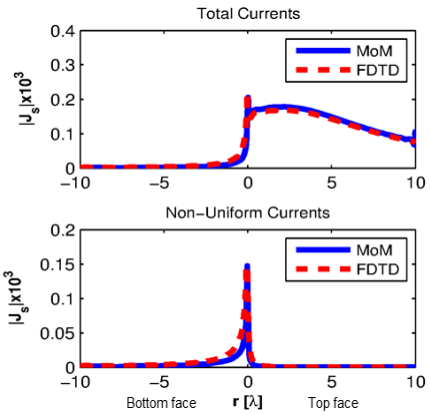

Fig. 7. Wedge surface currents for TM_z polarization of above scenario, (Top) total currents, (Bottom) fringe (non-uniform) currents, α=270°, ρ_0=60 m, φ_0=70°, ρ=20 m, f=30 MHz Solid: MoM, Dashed: FDTD (left and right portions belong to the bottom and top surfaces, respectively).

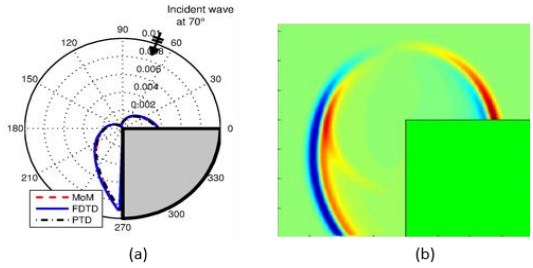

Fig. 8. (a) Fringe fields around the tip of the wedge; Dashed: MoM, Solid: FDTD, Dashed-dotted: PTD (TE_z pol, SSI, α=270°, ρ_0=60 m, φ_0=70°, ρ=20 m, f=30 MHz); (b) a time-domain FDTD snapshot showing broad-band fringe fields.

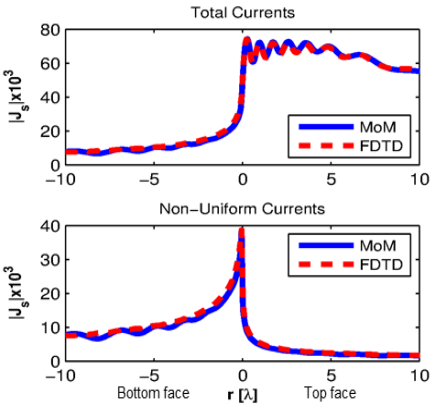

Fig. 9. Wedge surface currents for TE_z polarization of above scenario, (Top) total currents, (Bottom) fringe (non-uniform) currents, α=270°, ρ_0=60 m, φ_0=70°, ρ=20 m, f=30 MHz Solid: MoM, Dashed: FDTD (left and right portions belong to the bottom and top surfaces, respectively).

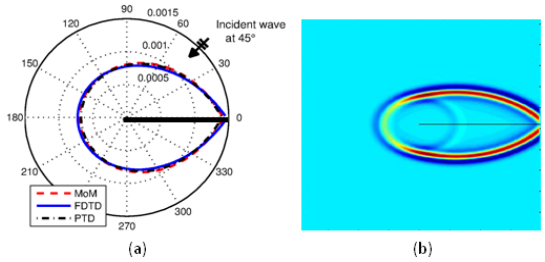

Fig. 10. (a) Fringe fields around the tip of the wedge; Dashed: MoM, Solid: FDTD, Dashed-dotted: PTD (TM_z pol, SSI, α=360°, ρ_0=70 m, φ_0=45°, ρ=20 m, f=30 MHz); (b) a time-domain FDTD snapshot.

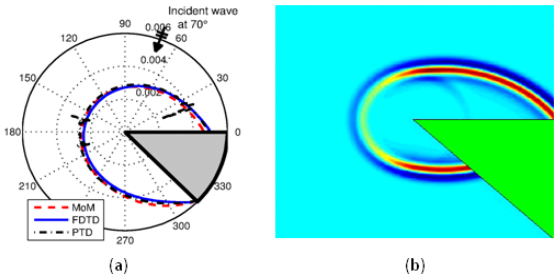

Fig. 11. (a) Fringe fields around the tip of the wedge; Dashed: MoM, Solid: FDTD, Dash-dot: PTD (SSI, TM_z pol, α=315°, ρ_0=60 m, φ_0=70°, ρ=5 m, f=30 MHz); (b) a time-domain FDTD snapshot.

V. CONCLUSIONS

For the first time in the literature, a novel, FDTD diffraction method is introduced for the simulation of fringe currents and fringe waves around a PEC wedge. Fringe currents and fringe waves are presented both in the frequency and time domains. The validity of the proposed method and the verification of the accuracy of the results are done using PTD and MoM generated fringe currents and fields.

Note that, using geometric averaging yields better performance for collocating electric and magnetic fields [14] and the accuracy may be increased. Also, the rectangular grid used in the standard FDTD algorithm limits the accuracy, especially for the TE polarization [15]. This limitation can be removed by using FDTD algorithms based on conformal cells [16]. Note also that, the FDTD-extracted fringe currents and fringe waves further demonstrate the argument on the modified theory of physical optics (MTPO) in [17].

REFERENCES

[1] H. Macdonald, "The effect produced by an obstacle on a train of electric waves," *Philosophical Transactions of the Royal Society A: Mathematical, Physical and Engineering Sciences*, vol. 212, no. 484-496, pp. 299-337, 1913.

[2] P. Ufimtsev, *Fundamentals of the Physical Theory of Diffraction*. Hoboken, N.J.: Wiley-Interscience, 2007.

[3] P. Ufimtsev, A. Terzuoli, and R. Moore, *Theory of Edge Diffraction in Electromagnetics*. Raleigh, NC: SciTech, 2009.

[4] F. Hacivelioglu, L. Sevgi, and P. Ufimtsev, "Wedge diffracted waves excited by a line source: Exact and asymptotic forms of fringe waves," *IEEE Trans. Antennas Propag.*, vol. 61, no. 9, pp. 4705-4712, Sept. 2013.

[5] G. Apaydin, F. Hacivelioglu, L. Sevgi, and P. Ufimtsev, "Wedge diffracted waves excited by a line source: Method of moments (mom) modeling of fringe waves," *IEEE Trans. Antennas Propag.*, vol. 62, no. 8, pp. 4368-4371, Aug. 2014.

[6] G. Cakir, L. Sevgi, and P. Ufimtsev, "FDTD modeling of electromagnetic wave scattering from a wedge with perfectly reflecting boundaries: Comparisons against analytical models and calibration," *IEEE Trans. Antennas Propag.*, vol. 60, no. 7, pp. 3336-3342, July 2012.

[7] G. Stratis, V. Anantha, and A. Taflove, "Numerical calculation of diffraction coefficients of generic conducting and dielectric wedges using FDTD," *IEEE Trans. Antennas Propag.*, vol. 45, no. 10, pp. 1525-1529, Oct. 1997.

[8] V. Anantha and A. Taflove, "Calculation of diffraction coefficients of three-dimensional infinite conducting wedges using FDTD," *IEEE Trans. Antennas Propag.*, vol. 46, no. 11, pp. 1755-1756, Nov. 1998.

[9] M. A. Uslu and L. Sevgi, "Matlab-based virtual wedge scattering tool for the comparison of high frequency asymptotics and fdtd method," *The Applied Computational Electromagnetics Society*, vol. 27, no. 9, 2012.

[10] M. A. Uslu, G. Apaydin, and L. Sevgi, "Double tip diffraction modeling: Finite difference time domain vs. method of moments," *IEEE Trans. Antennas Propag.*, vol. 62, no. 12, pp. 6337-6343, Dec. 2014.

[11] J. Bowman, T. Senior, and P. Uslenghi, *Electromagnetic and Acoustic Scattering by Simple Shapes*. New York: Hemisphere, 1987.

[12] F. Hacivelioglu, L. Sevgi, and P. Y. Ufimtsev, "On the numerical evaluation of diffraction formulas for the canonical wedge scattering problem," *IEEE Antennas Propag. Mag.*, vol. 55, no. 5, pp. 257-272, Oct. 2013.

[13] K. Yee, "Numerical solution of initial boundary value problems involving Maxwell;s equations in isotropic media," *IEEE Trans. Antennas Propag.*, vol. 14, no. 3, pp. 302-307, May 1966.

Mehmet Alper USLU received the B.S., M.S., and Ph.D. degrees in Electronics and Communications engineering from Dogus University, Istanbul, Turkey, in 2010, 2011, and 2015, respectively. His research interests are diffraction theory, radar system design, computational electromagnetics, RF Microwave circuits and systems, EMC, Digital Signal Processing Algorithms, Realtime/ Embedded Software Development, Radar Cross Section modeling. He has been with NETAS since 2012.

Gökhan Apaydin received the B.S., M.S., and Ph.D. degrees in Electrical and Electronics Engineering from Bogazici University, Istanbul, Turkey, in 2001, 2003, and 2007, respectively. He was a Teaching and Research Assistant with Bogazici University from 2001 to 2005; he was a Project Engineer with the University of Technology Zurich, Zurich, Switzerland, from 2005 to 2010; he was with Zirve University, Gaziantep, Turkey from 2010 to 2016; and he was a Visiting Associate Professor at the Department of ECE, University of Illinois at Urbana–Champaign, Champaign, IL, USA, in 2015. He has been involved with complex electromagnetic problems and systems. His research interests include analytical and numerical methods (FEM, MoM, FDTD, and SSPE) in electromagnetics (especially on electromagnetic computation of wave propagation, diffraction modeling, and related areas).

Levent Sevgi received the Ph.D. degree from Istanbul Technical University (ITU), Turkey, and Polytechnic Institute of New York University, Brooklyn, in 1990. Prof. Leo Felsen was his Advisor. He was with ITU (1991-1998); the Scientific and Technological Council of Turkey–Marmara Research Institute, Gebze/Kocaeli (1999-2000); Weber Research Institute/Polytechnic University in New York (1988-1990); the Scientific Research Group of Raytheon Systems, Canada (1998-1999); the Center for Defense Studies, ITUVSAM (1993-1998) and (2000-2002); the Department of ECE, UMASS Lowell, MA, USA (2012-2013) for his sabbatical term; and Dogus University (2001-2014). Since 2014, he has been with Okan University, Istanbul. He has been involved with complex electromagnetic problems and systems for nearly 30 years.